2011

Cholesterol Sensitivity of KIR2.1 Is Controlled by a Belt of Residues around the Cytosolic Pore

Avia Rosenhouse-Dantsker
University of Illinois at Chicago, dantsker@uic.edu

Diomedes E. Logothetis
Virginia Commonwealth University

Irena Levitan
University of Illinois at Chicago

Cholesterol Sensitivity of KIR2.1 Is Controlled by a Belt of Residues around the Cytosolic Pore

Avia Rosenhouse-Dantsker,[†*] Diomedes E. Logothetis,[‡] and Irena Levitan[†]
[†]Pulmonary Section, Department of Medicine, University of Illinois at Chicago, Chicago, Illinois; and [‡]Department of Physiology and Biophysics, Virginia Commonwealth University School of Medicine, Richmond, Virginia

ABSTRACT Kir channels play an important role in setting the resting membrane potential and modulating membrane excitability. A common feature of several Kir channels is that they are regulated by cholesterol. Yet, the mechanism by which cholesterol affects channel function is unclear. We recently showed that the cholesterol sensitivity of Kir2 channels depends on several CD-loop residues. Here we show that this cytosolic loop is part of a regulatory site that also includes residues in the G-loop, the N-terminus, and the connecting segment between the C-terminus and the inner transmembrane helix. Together, these residues form a cytosolic belt that surrounds the pore of the channel close to its interface with the transmembrane domain, and modulate the cholesterol sensitivity of the channel. Furthermore, we show that residues in this cluster are correlated with residues located in the most flexible region of the G-loop, the major cytosolic gate of Kir2.1, implying that the importance of these residues extends beyond their effect on the channel's cholesterol sensitivity. We suggest that the residues of the cholesterol sensitivity belt are critical for channel gating.

INTRODUCTION

Inwardly rectifying K^+ (Kir) channels constitute a major class of potassium channels that play critical roles in the maintenance of membrane potential and potassium homeostasis by regulating multiple cellular functions, including membrane excitability, heart rate, and vascular tone (1–3). Among these, Kir2.1 (IRK1) is the first member of the Kir2 subfamily of constitutively active, strongly inwardly rectifying K^+ channels. Kir2.1 is a component of the inward rectifier current IK_1, which provides substantial repolarizing current during the terminal repolarization phase of the cardiac action potential and is the primary conductance controlling the diastolic membrane potential (4,5). Furthermore, Kir2 channels are also critically involved in regulating the excitability and contraction of smooth muscle cells (6) and in maintaining membrane potential under resting conditions in endothelial cells (7,8). Kir2 channels have also been suggested to be one of the primary flow sensors (8). We previously showed that Kir2 channels are suppressed by elevation of membrane cholesterol and enhanced by cholesterol depletion, which suggests that the cholesterol sensitivity of these channels may play a major role in an array of physiological functions (9–11).

Cholesterol is one of the major lipid components of the plasma membrane in mammalian cells. Although cholesterol is essential for cell function and growth, its excess is associated with multiple pathological conditions (12–14), including the development of cardiovascular disease (15–17). Over the years, multiple types of ion channels have been shown to be affected by cholesterol (18–20). These include different types of K^+ channels (9,10,21–24), Ca^{+2} channels (25–29), Na^+ channels (30,31), and Cl^- channels (32,33). Recently, we showed that within the family of inwardly rectifying potassium channels, in addition to Kir2 channels, representative members of all other subfamilies of Kir channels are also sensitive to cholesterol (34). Yet, the mechanisms underlying cholesterol regulation of membrane proteins in general and of ion channels in particular are poorly understood.

In our earlier studies, we showed that cholesterol levels have no effect on the unitary conductance and only little effect on the open probability of the channels (10). We thus hypothesized that cholesterol modulates the function of Kir2 channels by stabilizing their closed state. Furthermore, we recently showed that mutations of three residues in the pore-facing CD loop of the cytosolic domain of Kir2.1, N216, K219, and L222 affect the sensitivity of the channel to cholesterol (11). The importance of the CD loop to cholesterol sensitivity extends beyond the Kir2 family. As we previously showed (34), corresponding mutations in the CD loop suppress the cholesterol sensitivity of Kir2.1 and Kir3.4* channels. Of interest, the same CD loop residues also play a critical role in regulating the function of different Kir channels by other modulators, including sodium (35–38) and $PI(4,5)P_2$ (39–41). In this study, we identify a belt of residues surrounding the cytoplasmic pore that controls the sensitivity of Kir2.1 channels to cholesterol. Furthermore, using docking analysis and the database of relevant crystallographic structures (42–48), we distinguish between the possibilities of direct and allosteric effects, and implicate the cholesterol sensitivity belt residues in channel gating.

Submitted October 8, 2010, and accepted for publication November 23, 2010.

*Correspondence: dantsker@uic.edu

Editor: Michael Pusch.

0006-3495/11/01/0381/9 $2.00

doi: 10.1016/j.bpj.2010.11.086

MATERIALS AND METHODS

Expression of recombinant channels in *Xenopus* oocytes

Point mutations were generated with the use of the Quickchange site-directed mutagenesis kit (Stratagene, LaJolla, CA). cRNAs were transcribed in vitro with the Message Machine kit (Ambion, Austin, TX). Oocytes were isolated and microinjected as previously described (49). Expression of channel proteins in *Xenopus* oocytes was accomplished by injecting the desired amount of cRNA. Oocytes were injected with 0.5 ng cRNA of the channel. All oocytes were maintained at 17°C. Two-electrode voltage-clamp recordings were performed 1 day after injection.

Cholesterol enrichment of *Xenopus* oocytes

Treatment of *Xenopus* oocytes with a mixture of cholesterol and lipids has been shown to increase the cholesterol/phospholipid molar ratio of the plasma membrane of oocytes (50). Thus, to enrich the oocytes with cholesterol, we used a 1:1:1 (wt/wt/wt) mixture containing cholesterol, porcine brain L-α-phosphatidylethanolamine (PE), and 1-palmitoyl-2-oleoyl-*sn*-glycero-3-phospho-L-serine (PS) (Avanti Polar Lipids, Birmingham, AL). The mixture was evaporated to dryness under a stream of nitrogen. The resultant pellet was suspended in a buffered solution consisting of 150 mM KCl and 10 mM Tris/HEPES at pH 7.4, and sonicated at 80 kHz in a bath sonicator (Laboratory Supplies, Hicksville, NY). The *Xenopus* oocytes were then treated with cholesterol for 1 h.

Two-electrode voltage-clamp recording and analysis

Whole-cell currents were measured by means of a conventional two-microelectrode voltage clamp with a GeneClamp 500 amplifier (Axon Instruments, Union City, CA) as previously described (49). A high-potassium (HK) solution (in mM: 96 KCl, 1 NaCl, 1 $MgCl_2$, 5 KOH/HEPES, pH 7.4) was used to superfuse the oocytes. Basal currents represent the difference of inward currents obtained (at −80 mV) in the presence of 3 mM $BaCl_2$ in HK solution from those in the absence of Ba^{2+}. A minimum of two batches of oocytes were tested for each normalized recording shown. Recordings from different batches of oocytes were normalized to the mean of whole-cell basal currents obtained from control untreated oocytes. The mean of each batch of control untreated oocytes was normalized to one. Statistics (i.e., the mean and standard error of the mean) of each construct were calculated from all of the normalized data recorded from different batches of oocytes.

Molecular docking of cholesterol to Kir2.1

Molecular docking was carried out with the use of ArgusLab (51,52). The model of the channel used (KDB database ID H011) (53,54) was based on the chimera between the cytosolic domain of Kir3.1 and the TM domain of KirBac1.3 (PDB ID 2QKS; resolution 2.2 Å) (47). The L222 residues in the four subunits of the channel were grouped so as to define the center of the binding site box. The size of the binding site box was set around the L222 binding center at its maximal allowable value of $60 \times 60 \times 60$ Å^3. Possible binding sites of cholesterol were searched within the binding-site box. An exhaustive search was carried out using grids at a resolution of 0.4 Å, and a flexible ligand-docking mode was employed. The maximal number of poses was set at 150. To achieve high accuracy (52), all 135 possible poses that were identified by the program were included in the analysis. Clustering analysis was carried out with the use of a *k*-medoid algorithm, a classic partitioning technique that groups *n* objects into *k* clusters. Each pose was associated with the closest center-pose of a cluster as determined by a Euclidean distance metric.

Analysis of crystallographic structures of the cytosolic domains of eukaryotic Kir channels

In recent years, the crystallographic structures of several inwardly rectifying potassium channels have been determined. These include the complete prokaryotic Kir channels (KirBac1.1 (42) and KirBac3.1 (43)); the cytosolic domains of several eukaryotic channels (Kir2.1 (44), Kir3.1 (44,45), and Kir3.2 (46)); the chimera between the transmembrane (TM) domain of the prokaryotic KirBac3.1 channel and the cytosolic domain of the eukaryotic Kir3.1 channel (47); and, more recently, the crystallographic structure of Kir2.2 (48). These structures serve as the basis for models of Kir channels (11,38,54–56). For the analysis, we downloaded from the Protein Data Bank (PDB) all currently available crystallographic structures of symmetrical cytosolic domains of eukaryotic Kir channels. The structures were used without any modeling. These included the following eight structures of members of the Kir2 and Kir3 subfamilies: 1n9p (cytosolic domain of Kir3.1) (45), 1u4e (cytosolic domain of Kir3.1) (44), 1u4f (cytosolic domain of Kir2.1) (44), 2e4f (cytosolic domain of Kir3.2) (46), 2qks (opened and closed chimeras of the TM domain of KirBac1.3 and cytosolic domains of Kir3.1) (47), 3k6n (Kir3.1S225E) (57), and 3jyc (Kir2.2) (48). Due to flexibility of some regions, some of the structures did not include all of the residues examined in this study. Therefore, the analysis in each case (Fig. 5, and Table S1, Table S2, Table S3, and Table S4 in the Supporting Material) was based on all the structures in which the residues examined were present. Distances were measured between equivalent atoms in two opposite-facing subunits of the channel using the PyMOL Molecular Graphics System, version 1.1 (Schrödinger, LLC, Portland, OR), and the correlations (R) between these distances for different atoms were calculated (see Fig. 5, Table S2, Table S3, and Table S4). Correlations (R) and their significance (P) were calculated using the linear fit tool in the data analysis and graphing software Origin (OriginLab, Northampton, MA). A correlation was regarded as significant with $P \leq 0.05$.

Determination of the most flexible region in a cytosolic loop in Kir channels

We determined the intrinsic flexibility of cytosolic residues in Kir channels (Table S1) by examining the variations in the distances between their backbone Cα atoms in two opposite-facing subunits, using all available crystallographic structures that included symmetrical cytosolic domains of eukaryotic Kir channels as listed above. Furthermore, when possible, we also examined the variations in the distances between the side-chain Cβ atoms in two opposite-facing subunits.

RESULTS AND DISCUSSION

Identification of critical residues for the cholesterol sensitivity of Kir2.1

As noted in the Introduction, we recently showed that three residues in the CD loop affect the cholesterol sensitivity of Kir2.1 (11,34). Among these, the L222I mutation abrogates cholesterol sensitivity. In accord with this observation, the reverse mutation of the equivalent residue in Kir2.3 (a channel that exhibits reduced cholesterol sensitivity compared with Kir2.1 (10,58)), I214L, increases the sensitivity of Kir2.3 to cholesterol (11). Although the two

channels differ in just one residue in the CD loop, outside the CD loop, the channels exhibit >40 differences in the modeled cytosolic domain, which we investigated in this study (see Fig. S1).

Critical residues for cholesterol sensitivity of Kir2.1 in proximity to the CD loop

Surrounding the CD loop itself, there are six residues that differ between Kir2.1 and Kir2.3 in both the N- and C-termini (Fig. 1 *A*). We thus mutated each of these residues to the corresponding residues in Kir2.3, and examined the effect of the mutations on the cholesterol sensitivity of Kir2.1.

The beginning of the N-terminus of crystallized inwardly rectifying potassium channels is missing from their structures. Thus, the first residue in the model of Kir2.1 is residue number 45 of the N-terminus. Across from the CD loop (Fig. 1 *A*), there are two residues, close to the beginning of the modeled N-terminus, that differ between Kir2.1 and Kir2.3: an aspartate at position 51 (D51) and a histidine at position 53 (H53; see Fig. S1). In Kir2.3 the equivalent residue to D51 is an asparagine and the equivalent residue to H53 is a glutamine (Fig. S1). Thus, we examined the effects of the D51N and H53Q mutations on the cholesterol sensitivity of Kir2.1. As can be seen in Fig. 1 *B* and Fig. S2, both residues affected cholesterol sensitivity, albeit to different extents: the H53Q mutation abrogates cholesterol sensitivity, and D51N mutation reduced the cholesterol sensitivity of the channel by 43%.

Within the C-terminus, the residues that differ between Kir2.1 and Kir2.3 in the proximity of the CD-loop include residues in the G-loop and in the segment that links the C-terminus to the inner TM helix. First, we examined the part of the linker between the inner TM helix and the C-terminus. We previously showed that mutations of K182, K185, and K187 to a glutamine do not affect the cholesterol sensitivity of the channel (11). Apart from K185, the linker between the inner TM helix of the channel and its C-terminus is conserved among Kir2 channels up to R189. The next segment includes three differences between Kir2.1 and Kir2.3 at positions 190, 191, and 194 (Fig. S1). We thus examined the effect of the N190A, E191Q, and V194L mutations on the cholesterol sensitivity of Kir2.1. As shown in Fig. 1 *C*, both E191Q and V194L abrogated the cholesterol sensitivity of the channel; in both cases there was no significant difference between control and cholesterol-treated oocytes (for E191Q, $P = 0.94$; for V194, $P = 0.39 > 0.05$). The N190A mutation, on the other hand, did not affect cholesterol sensitivity (see representative traces in Fig. S2). It is noteworthy that whereas N190 is located closer to the TM domain, E191 and V194 are located close to K219 and N216 of the CD loop, respectively (Fig. 1 *A*).

Adjacent to the CD loop is also the HI or G-loop, which includes residues 300–310. The G-loop is highly conserved in Kir channels, and the only residue in the G-loop that is not

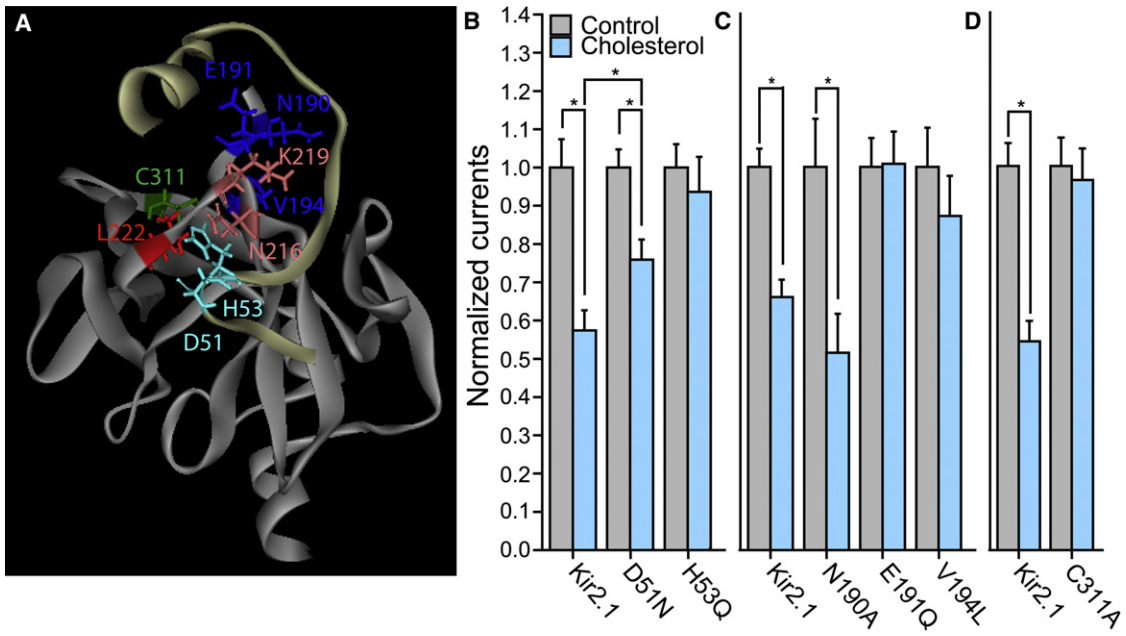

FIGURE 1 (*A*) Model of the CD loop in a Kir2.1 subunit and its surrounding residues that differ between Kir2.1 and Kir2.3. These include N190, E191, and V194 in the segment that connects the C-terminus with the inner TM helix, C311 of the G-loop, and D51 and H53 in a short segment from an adjacent subunit. Also shown are L222, N216, and K219 of the CD loop. (*B–D*) Whole-cell basal currents recorded in *Xenopus* oocytes at −80 mV, showing the effect of cholesterol enrichment on (*B*) Kir2.1 and the mutants D51N and H53Q; (*C*) Kir2.1 and the single mutants N190A, E191Q, and V194L; and (*D*) Kir2.1 and its C311A mutant. Significant difference in *B–D* is indicated by an asterisk (*$P \leq 0.05$).

conserved among Kir2 channels is C311, whose position relative to the CD loop is shown in Fig. 1 *A*. C311 was previously mutated to an alanine, a serine, and an arginine to investigate its contribution to the gating properties of the channel (41). In Kir2.3, which exhibits reduced cholesterol sensitivity compared with Kir2.1, there is an alanine in the equivalent position to C311 of Kir2.1 (Fig. S1). We thus tested the effect of the C311A mutation on the cholesterol sensitivity of Kir2.1. As can be seen in Fig. 1 *D* and Fig. S2, the C311A mutation results in loss of cholesterol sensitivity of the channel.

Screening the effect of the additional differences between the modeled cytosolic domain residues of Kir2.1 and Kir2.3 on cholesterol sensitivity of Kir2.1

In addition to the residues we examined, there are 42 additional differences between Kir2.1 and Kir2.3 in the model of the cytosolic domain of Kir2.1 (Fig. S1). To investigate the effect of these differences on cholesterol sensitivity in an efficient manner, we grouped the residues into eight groups (see Fig. 2, *A* and *B*). We then made multiple point mutations of all the different residues in Kir2.1 and Kir2.3 within each group, mutating each of them to the equivalent residues in Kir2.3. As can be seen in Fig. 2 *C*, none of these mutations abrogated the cholesterol sensitivity of the channel. This does not imply that there are no additional residues in the cytosolic domain that affect the cholesterol sensitivity of the channel; however, this result does suggest that the difference between Kir2.1 and Kir2.3 in terms of their cholesterol sensitivity originates from the differences in the residues in the CD loop and in its proximal surrounding regions.

Residues whose mutation affects the cholesterol sensitivity of Kir2.1 form a belt around the cytosolic pore of the channel

When we highlight the positions of the cytosolic residues that we identified in the model (Fig. 3, *A* and *B*, it can be clearly seen that these residues form a belt around the pore of the channel close to the TM domain. E191 and V194, in the linker between the C-terminus and the inner TM helix, are shown in blue in Fig. 3. D51 and H53 in the N-terminus are shown in cyan. C311 in the G loop is

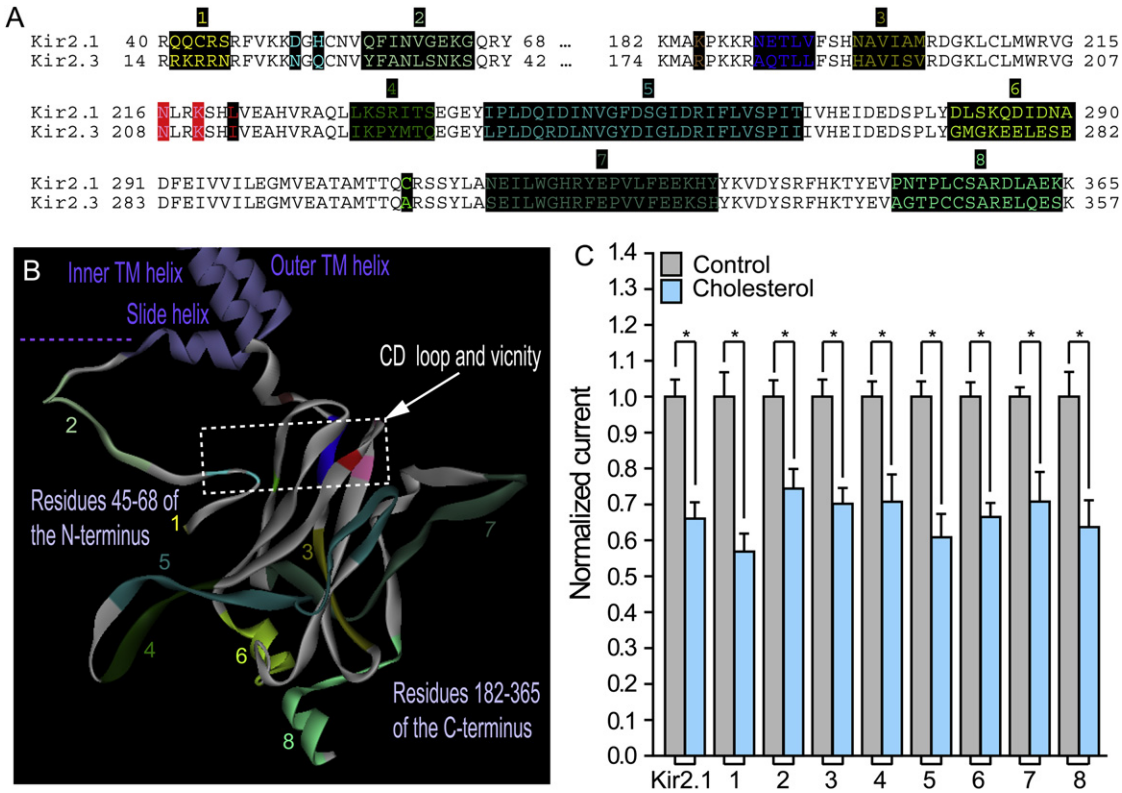

FIGURE 2 (*A*) Sequence alignment of residues 40–68 located in the N-terminus of Kir2.1 with the equivalent residues in Kir2.3 (residues 14–42), and of the modeled C-terminus residues 182–365 of Kir2.1 with the corresponding residues in Kir2.3 (residues 174–357). Highlighted in black on the sequence alignment are segments that include residues that differ between Kir2.1 and Kir2.3. (*B*) A model of the cytosolic domain of one subunit of Kir2.1, showing segments 1–8 that correspond to the groups of residues labeled 1–8 in panel *A*. Also shown are the CD loop and its proximal residues whose mutation affects the channel's cholesterol sensitivity. The colors correspond to the colors in the alignment in panel *A*. (*C*) Whole-cell basal currents recorded in *Xenopus* oocytes at −80 mV, showing the effect of cholesterol enrichment on Kir2.1 and on each of the multiple mutants 1–8 that include mutations of the segments shown in panel *A* to the corresponding segments in Kir2.3. Significant difference is indicated by an asterisk (*$P < 0.05$).

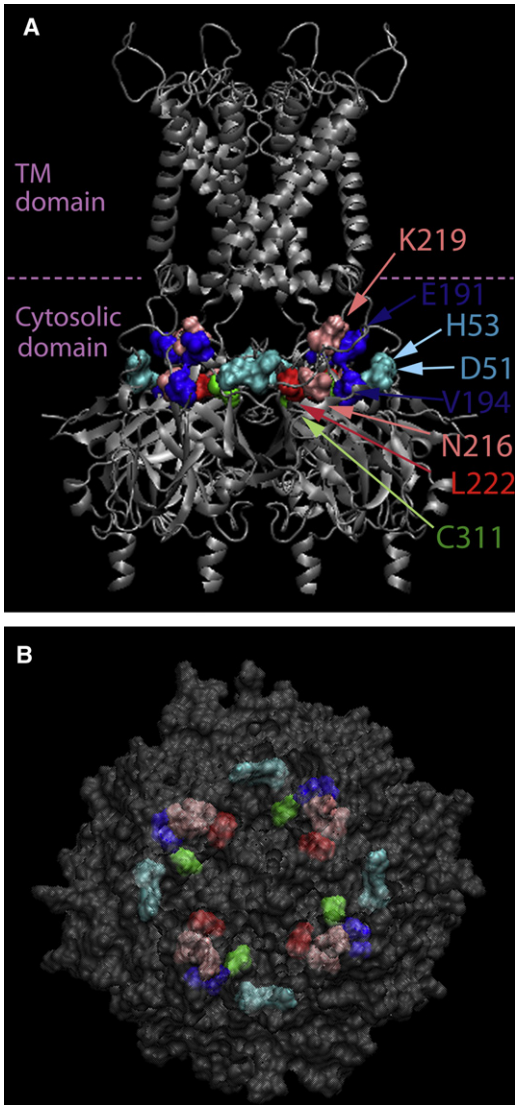

FIGURE 3 (*A*) Side view of a model of Kir2.1 that includes all four subunits. Shown in the model are the residues whose mutation affects cholesterol sensitivity: D51 and H53 (*cyan*), E191 and V194 (*blue*), N216 and K219 (*pink*), L222 (*red*), and C311 (*green*). (*B*) Top view of the model of Kir2.1 from the membrane, showing the cholesterol sensitivity belt formed by the residues whose mutation affects the cholesterol sensitivity of the channel.

shown in green. Also shown are residues that we identified previously (11): L222 in red, and N216 and K219 in pink.

Why are the cytosolic residues that affect cholesterol sensitivity arranged in a structured manner?

In general, cholesterol may regulate ion channels either directly or indirectly through interactions with other modulators (20). Our recent studies demonstrated, however, that cholesterol regulates purified prokaryotic Kir when the channels are incorporated into liposomes, indicating that no intermediate modulators are required (59). Furthermore, we also showed that cholesterol-induced suppression of Kir channels does not correlate with changes in membrane fluidity, as indicated by a comparative analysis of different sterols (59). Taken together, these studies suggest that cholesterol binds directly to the channel. With the residues that we identified to be critical for cholesterol sensitivity of the channel all clustered in the same region of the cytosolic domain, we next sought to determine whether the clustered residues constitute a cholesterol-binding site.

Identification of possible cytosolic cholesterol-binding sites

To identify possible cholesterol binding sites in the cytosolic domain of Kir2.1 that may include the residues of the cholesterol sensitivity belt, we screened for potential sites within a box of 60 $Å^3$ around the L222 residues of the four subunits of the channel, as depicted in Fig. 4 *A*. The result was 135 possible poses. We then examined each residue of the modeled cytosolic domain for the frequency of appearance in all 135 poses (Fig. S3 *A*). Of note, the majority of the residues that affect cholesterol sensitivity

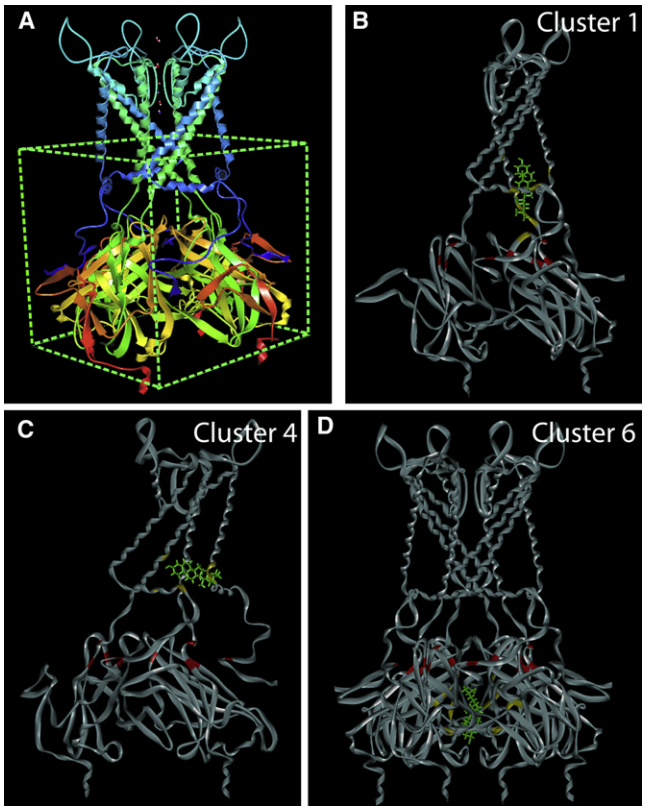

FIGURE 4 (*A*) The 60 $Å^3$ box around the L222 residues of the four subunits that defines the search area for possible cholesterol-binding sites. (*B–D*) Location of the cholesterol molecule in the center of clusters: (*B*) 1, (*C*) 4, and (*D*) 6. The residues that participate in the binding site and surround the cholesterol molecule are highlighted. Also shown are the residues of the cholesterol sensitivity belt that surround the cytosolic pore in proximity to the membrane.

(D51, H53, V194, N216, L222, and C311) did not appear in any of the poses.

To further investigate whether there is a correlation between the locations of the potential cytosolic binding sites and the residues of the cholesterol sensitivity belt, we grouped all of the poses in six clusters. The clusters and the similarity between each two poses are plotted in Fig. S3 *B*. Of interest, five of the clusters were located on the boundary between the cytosolic and the TM domains. As examples, the centers of clusters 1 and 4 are shown in Fig. 4, *B* and *C*. Cluster 6, on the other hand, suggested a possible binding site at the center of the cytosolic domain away from the TM domain, as depicted in Fig. 4 *D*. A complete picture of all six clusters, along with the residues that appear in the binding sites defined by the members of each cluster, and the percentage of poses in the cluster in which each residue appears, is provided in Fig. S4. These results show that the potential binding sites identified by the docking analysis would be either above (closer to the TM domain, clusters 1–5) or below (farther away from the TM domain, cluster 6) the location of the cholesterol sensitivity belt. Thus, there is no correspondence between any of these possible cytosolic cholesterol-binding sites and the location of the residues that define the cholesterol sensitivity belt, suggesting that the cholesterol sensitivity belt does not form a cholesterol-binding site.

This conclusion is further corroborated by a comparison between the residues included in the cholesterol sensitivity belt with the known cholesterol recognition/interaction amino acid consensus (CRAC) (60). The CRAC motif is -L/V-(X)(1–5)-Y-(X)(1–5)-R/K-, where (X)(1–5) represents between one and five residues of any amino acid (60,61). Accordingly, there is no similarity between the residues identified in this study and known cholesterol-binding motifs.

We therefore proceeded to investigate an alternative possibility. As noted in the Introduction, on the basis of single-channel recordings, cholesterol is expected to stabilize the closed state of Kir2.1 (10), thereby affecting the ability of the channel to gate. We thus examined the relationship between the residues in the cholesterol sensitivity belt and channel gating.

Cholesterol sensitivity belt residues and critical residues in the G-loop

Within the cytosolic domain of Kir channels, the HI- or G-loop has been proposed to act as a cytosolic gate (1,44,47,62). This loop forms a girdle around the central pore axis in proximity to the TM domain. On the basis of a variety of crystal structures and functional data, it has been shown that changes in pore size at the G-loop are achieved via rigid-body movement of the cytosolic domain (47,63), and when local changes occur in the structure of the G-loop due to its intrinsic flexibility (44,46–48,62). These variations in the conformation of Kir channels at the G-loop highlight its importance as a critical cytosolic gate. Moreover, evidence for the role of the G-loop in KirBac3.1 further supports its role as an actual gate in the cytoplasmic domain (62). To date, eight structures of the symmetrical cytosolic domains of different members of the eukaryotic Kir2 and Kir3 subfamilies have been crystallized (see Materials and Methods). Despite the different crystallization conditions employed in different studies, the overall structural elements of the cytoplasmic region seem to be highly conserved in the Kir channel family (44,46). The primary differences are observed at the flexible loops, where significant changes occur during gating (44,46,62). These differences may reflect fluctuations of the cytosolic domain along the pathway that connects the open and closed conformations of the channel (48).

To examine the relationship between the residues of the cholesterol sensitivity belt and residues that are important for gating in the G-loop, we first used the group of crystal structures of the cytosolic domains of Kir channels to identify the most flexible region of the G-loop, as these residues are expected to be critical for channel gating. As can be seen in Table S1, the most flexible region of the G-loop is located at its apex, and includes positions equivalent to the following Kir2.1 residues: E303, A304, T305, A306, and M307 (Fig. 5 *A*). Of note, the equivalent positions to A306 (44) and M307 (47) have been associated with the most constricted parts of the G-loop, which are required to move significantly during gating. In addition, residues at the equivalent positions to E303 and T305 in KirBac3.1 have been identified among the residues that exhibit the highest changes in accessibility during gating (62).

We next examined whether the selectivity belt residues are correlated with any of the residues in the most flexible region of the G-loop. Our analysis shows that all of the residues that belong to the cholesterol sensitivity belt are correlated (or anticorrelated) with at least one of the G-loop apex residues (Fig. 5, *B–F*, Table S2, and Table S3), i.e., E303 or M307. Fig. 5, *B–F*, depict representative correlation plots between the residues in the sensitivity belt that completely abrogated cholesterol sensitivity and the apex residues of the G-loop. As can be seen in the figure, H53 is correlated with M307 (Fig. 5 *B*), E191 is anticorrelated with M307 (Fig. 5 *C*), V194 is anticorrelated with E303 (Fig. 5 *D*), L222 is correlated with E303 (Fig. 5 *E*), and C311 is correlated with M307 (Fig. 5 *F*). The results of our analysis of possible correlations between the cholesterol sensitivity belt residues and the apex G-loop residues are summarized in Table S2 and Table S3. As a comparison, we also examined the relationship between residues outside but in close proximity to the sensitivity belt and the apex G-loop residues. As can be seen in Table S4, no significant correlation was found between any of the apex G-loop residues and Q57 or N190 ($P > 0.05$) (1), whose mutation did not affect

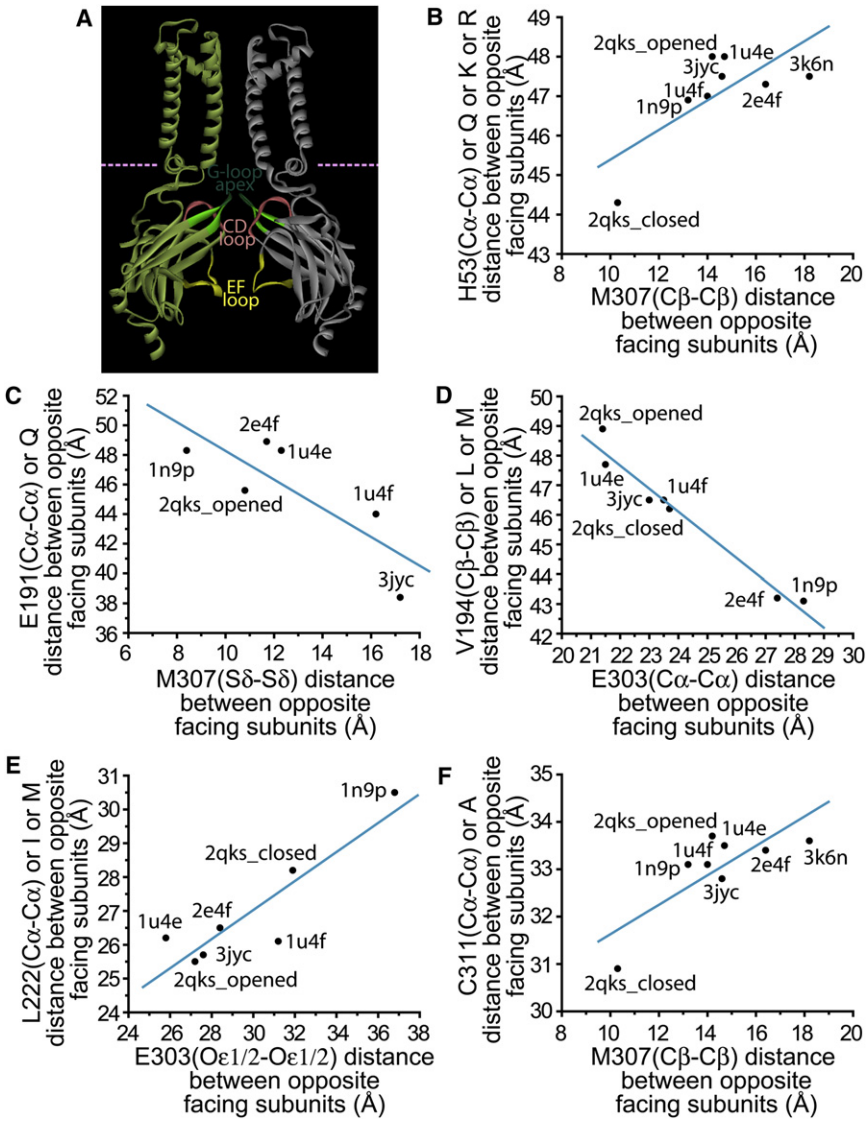

FIGURE 5 (*A*) Model of Kir2.1 showing the cytosolic pore facing loops in two opposite-facing subunits. Within the G-loop, its apex residues are shown in a darker shade. Also shown are the CD- and EF-loops. (*B–F*) Correlations based on crystallographic structures of Kir channels between the following distances: (*B*) The distance between Met307(Cβ) of two opposite-facing subunits and the distance between H53(Cα) (or K or Q or R) of two opposite subunits. The correlation and its significance are R = 0.73, $P = 4 \times 10^{-2}$. (*C*) The distance between Met307(Sδ) of two opposite-facing subunits and the distance between E191(Cα) (or Q) of two opposite subunits. The correlation and its significance are R = −0.81, $P = 5 \times 10^{-2}$. (*D*) The distance between Glu303 (Cα) of two opposite-facing subunits and the distance between V194(Cβ) (or L or M) of two opposite subunits. The correlation and its significance are R= −0.98, $P < 1 \times 10^{-4}$. (*E*) The distance between Glu303(O$\varepsilon_{1/2}$) of two opposite-facing subunits and the distance between L222 (Cα) (or I or M)) of two opposite subunits. Because glutamates have two equivalent carboxyl oxygen atoms, the distance between Glu303(O$\varepsilon_{1/2}$) of two opposite-facing subunits is defined as the minimal distance of the two possibilities: Oε_1-Oε_1 and Oε_2-Oε_2. The correlation and its significance are R = 0.90, $P = 6 \times 10^{-3}$. (*F*) The distance between Met307(Cβ) of two opposite facing subunits and the distance between C311 (Cα) of two opposite subunits. The correlation and its significance are R = 0.79, $P = 2 \times 10^{-2}$. In *B–F*, the numbers of the residues mentioned refer to the numbering in Kir2.1. In the case of crystallographic structures of other Kir channels, residues at equivalent positions were used. Cα is the central backbone carbon atom to which the side-chain of the amino acid is attached, and Cβ is the side-chain carbon attached to the Cα.

the cholesterol sensitivity of Kir2.1. This suggests that clustering of the residues in the sensitivity belt is a result of the correlation between these residues and the residues located at the apex of the G-loop.

Moreover, this correlation between the cholesterol sensitivity belt residues and the G-loop apex residues suggests a critical role for the sensitivity belt residues in gating. Notably, residues just outside the sensitivity belt are not correlated with these G-loop apex residues. Taken together with the notion that cholesterol stabilizes the closed state of the channel (based on our previous studies), our data suggest that the cytosolic belt residues control the cholesterol sensitivity of Kir2.1 by affecting its gating mechanism. Further structural studies, however, are needed to elucidate the exact conformational changes that underlie the effect of cholesterol on channel gating.

CONCLUSIONS

Although numerous ion channels are regulated by the level of membrane cholesterol, very little is known about the structure-function relationship of their cholesterol sensitivity. On the basis of differences in the cytosolic domain of Kir2.1 and Kir2.3, which differ significantly in their sensitivity to cholesterol (10,58), in this study we identified a group of residues that abrogate or significantly decrease the cholesterol sensitivity of the channel in the vicinity of L222 of the CD loop. Among these, in addition to L222, the residues whose mutation abrogated the cholesterol sensitivity of Kir2.1 include H53 of the N-terminus; E191 and V194, which are located in the link between the inner TM helix and the C-terminus; and C311 of the G-loop. Most importantly, these residues were not scattered randomly across the cytosolic domain of the channel but

formed a belt structure surrounding the cytosolic pore of the channel close to its interface with the membrane.

We then sought to determine why the residues that affect cholesterol sensitivity are arranged in a structured manner and not spread randomly across the channel. One possibility was that the residues of the cholesterol sensitivity belt interact with cholesterol directly. To investigate this possibility, we performed a molecular docking analysis to identify potential cholesterol-binding sites in the cytosolic domain of Kir2.1. The first clue that the cholesterol sensitivity belt does not form a cholesterol-binding site came from the observation that the majority of the residues that comprise the belt have not been identified in any of the potential cholesterol-binding sites. Furthermore, among the six representative clusters of potential binding sites, five clusters were located at the interface between the cytosolic and the TM domains, and were significantly above the plane of the cholesterol sensitivity belt, whereas the sixth suggested a possible binding site at the center of the cytosolic domain significantly below the plane of the belt. Thus, in the absence of correlation between any of these potential cytosolic cholesterol-binding sites and the location of the residues identified in this study as the cholesterol sensitivity belt, we conclude that the cholesterol sensitivity belt does not constitute a cholesterol-binding site.

We thus examined the implications of our findings in the context of Kir channel gating. Within the cytosolic domain, the major gate of Kir2.1 is located at the G-loop (44), which is regarded as the main region of the cytoplasmic pore where dilation and contraction occur. Thus, using a database of crystallographic structures that include the cytosolic domains of eukaryotic Kir channels, we searched for correlations between residues located in the most flexible region of the G-loop (i.e., its apex) and residues of the cholesterol sensitivity belt. Surprisingly, all of the residues of the cholesterol sensitivity belt were correlated (or anticorrelated) with residues located in the apex of the G-loop. In contrast, no significant correlation was found between the apex G-loop residues and residues that were just outside the selectivity belt. This observation clearly has implications beyond the scope of modulation of the channel by cholesterol. In fact, several of the residues of the cholesterol sensitivity belt overlap with residues that affect modulation of the channel by $PI(4,5)P_2$, a phosphoinositide required for channel activation. These include H53 (39), L222 (37), and C311 (41). The common denominator between $PI(4,5)P_2$ and cholesterol is that both affect channel gating: the first activates the channel, whereas the latter is expected to result in stabilization of its closed state. This suggests that the underlying reason for the clustering of the cholesterol sensitive residues in a belt that surrounds the pore of the channel in proximity to the membrane is the importance of these residues for Kir channel gating. Moreover, it is possible that the residues included in the cholesterol sensitivity belt couple events at the membrane interface to channel gating.

SUPPORTING MATERIAL

Four figures and four tables are available at http://www.biophysj.org/biophysj/supplemental/S0006-3495(10)-52-4-5.

We thank Heikki Vaananen and Sophia Gruszecki for oocyte preparation.

This work was supported by the National Institutes of Health (grants HL-073965 and HL-083298 to I.L., and HL-059949 and HL-090882 to D.E.L.).

REFERENCES

1. Bichet, D., F. A. Haass, and L. Y. Jan. 2003. Merging functional studies with structures of inward-rectifier K^+ channels. *Nat. Rev. Neurosci.* 4:957–967.
2. Kubo, Y., J. P. Adelman, …, C. A. Vandenberg. 2005. International Union of Pharmacology. LIV. Nomenclature and molecular relationships of inwardly rectifying potassium channels. *Pharmacol. Rev.* 57:509–526.
3. Nichols, C. G., and A. N. Lopatin. 1997. Inward rectifier potassium channels. *Annu. Rev. Physiol.* 59:171–191.
4. Hutter, O. F., and D. Noble. 1960. Rectifying properties of heart muscle. *Nature.* 188:495.
5. Sanguinetti, M. C., and M. Tristani-Firouzi. 2000. Delayed and inward rectifier potassium channels. *In* Cardiac Electrophysiology From Cell to Bedside, 3rd ed. D. P. Zipes and J. Jalife, editors. Elsevier/W.B. Saunders, Philadelphia. 79–85.
6. Zaritsky, J. J., D. M. Eckman, …, T. L. Schwarz. 2000. Targeted disruption of Kir2.1 and Kir2.2 genes reveals the essential role of the inwardly rectifying K^+ current in K^+-mediated vasodilation. *Circ. Res.* 87:160–166.
7. Olesen, S.-P., D. E. Clapham, and P. F. Davies. 1988. Haemodynamic shear stress activates a K^+ current in vascular endothelial cells. *Nature.* 331:168–170.
8. Fang, Y., G. Schram, …, I. Levitan. 2005. Functional expression of Kir2.x in human aortic endothelial cells: the dominant role of Kir2.2. *Am. J. Physiol. Cell Physiol.* 289:C1134–C1144.
9. Romanenko, V. G., G. H. Rothblat, and I. Levitan. 2002. Modulation of endothelial inward-rectifier K^+ current by optical isomers of cholesterol. *Biophys. J.* 83:3211–3222.
10. Romanenko, V. G., Y. Fang, …, I. Levitan. 2004. Cholesterol sensitivity and lipid raft targeting of Kir2.1 channels. *Biophys. J.* 87:3850–3861.
11. Epshtein, Y., A. P. Chopra, …, I. Levitan. 2009. Identification of a C-terminus domain critical for the sensitivity of Kir2.1 to cholesterol. *Proc. Natl. Acad. Sci. USA.* 106:8055–8060.
12. Kellner-Weibel, G., Y. J. Geng, and G. H. Rothblat. 1999. Cytotoxic cholesterol is generated by the hydrolysis of cytoplasmic cholesteryl ester and transported to the plasma membrane. *Atherosclerosis.* 146:309–319.
13. Yeagle, P. L. 1985. Cholesterol and the cell membrane. *Biochim. Biophys. Acta.* 822:267–287.
14. Yeagle, P. L. 1991. Modulation of membrane function by cholesterol. *Biochimie.* 73:1303–1310.
15. Kruth, H. S. 2001. Lipoprotein cholesterol and atherosclerosis. *Curr. Mol. Med.* 1:633–653.
16. Ross, R. 1999. Atherosclerosis—an inflammatory disease. *N. Engl. J. Med.* 340:115–126.
17. Steinberg, D. 2002. Atherogenesis in perspective: hypercholesterolemia and inflammation as partners in crime. *Nat. Med.* 8:1211–1217.
18. Maguy, A., T. E. Hebert, and S. Nattel. 2006. Involvement of lipid rafts and caveolae in cardiac ion channel function. *Cardiovasc. Res.* 69:798–807.
19. Levitan, I. 2009. Cholesterol and Kir channels. *IUBMB Life.* 61:781–790.
20. Levitan, I., Y. Fang, …, V. Romanenko. 2010. Cholesterol and ion channels. *Subcell. Biochem.* 51:509–549.

21. Bolotina, V., V. Omelyanenko, …, P. Bregestovski. 1989. Variations of membrane cholesterol alter the kinetics of Ca^{2+}-dependent K^+ channels and membrane fluidity in vascular smooth muscle cells. *Pflugers Arch.* 415:262–268.
22. Heaps, C. L., D. L. Tharp, and D. K. Bowles. 2005. Hypercholesterolemia abolishes voltage-dependent K^+ channel contribution to adenosine-mediated relaxation in porcine coronary arterioles. *Am. J. Physiol. Heart Circ. Physiol.* 288:H568–H576.
23. Martens, J. R., R. Navarro-Polanco, …, M. M. Tamkun. 2000. Differential targeting of Shaker-like potassium channels to lipid rafts. *J. Biol. Chem.* 275:7443–7446.
24. Martens, J. R., N. Sakamoto, …, M. M. Tamkun. 2001. Isoform-specific localization of voltage-gated K^+ channels to distinct lipid raft populations. Targeting of Kv1.5 to caveolae. *J. Biol. Chem.* 276:8409–8414.
25. Ambudkar, I. S. 2004. Cellular domains that contribute to Ca^{2+} entry events. *Sci. STKE.* 2004:pe32.
26. Bowles, D. K., C. L. Heaps, …, E. M. Price. 2004. Hypercholesterolemia inhibits L-type calcium current in coronary macro-, not microcirculation. *J. Appl. Physiol.* 96:2240–2248.
27. Lockwich, T. P., X. Liu, …, I. S. Ambudkar. 2000. Assembly of Trp1 in a signaling complex associated with caveolin-scaffolding lipid raft domains. *J. Biol. Chem.* 275:11934–11942.
28. Lundbaek, J. A., P. Birn, …, O. S. Andersen. 1996. Membrane stiffness and channel function. *Biochemistry.* 35:3825–3830.
29. Toselli, M., G. Biella, …, M. Parenti. 2005. Caveolin-1 expression and membrane cholesterol content modulate N-type calcium channel activity in NG108-15 cells. *Biophys. J.* 89:2443–2457.
30. Lundbaek, J. A., P. Birn, …, O. S. Andersen. 2004. Regulation of sodium channel function by bilayer elasticity: the importance of hydrophobic coupling. Effects of micelle-forming amphiphiles and cholesterol. *J. Gen. Physiol.* 123:599–621.
31. Wu, C. C., M. J. Su, …, Y. T. Lee. 1995. The effect of hypercholesterolemia on the sodium inward currents in cardiac myocyte. *J. Mol. Cell. Cardiol.* 27:1263–1269.
32. Levitan, I., A. E. Christian, …, G. H. Rothblat. 2000. Membrane cholesterol content modulates activation of volume-regulated anion current in bovine endothelial cells. *J. Gen. Physiol.* 115:405–416.
33. Romanenko, V. G., G. H. Rothblat, and I. Levitan. 2004. Sensitivity of volume-regulated anion current to cholesterol structural analogues. *J. Gen. Physiol.* 123:77–87.
34. Rosenhouse-Dantsker, A., E. Leal-Pinto, …, I. Levitan. 2010. Comparative analysis of cholesterol sensitivity of Kir channels: role of the CD loop. *Channels (Austin).* 4:63–66.
35. Ho, I. H., and R. D. Murrell-Lagnado. 1999. Molecular determinants for sodium-dependent activation of G protein-gated K^+ channels. *J. Biol. Chem.* 274:8639–8648.
36. Ho, I. H., and R. D. Murrell-Lagnado. 1999. Molecular mechanism for sodium-dependent activation of G protein-gated K^+ channels. *J. Physiol.* 520:645–651.
37. Zhang, H., C. He, …, D. E. Logothetis. 1999. Activation of inwardly rectifying K^+ channels by distinct PtdIns(4,5)P_2 interactions. *Nat. Cell Biol.* 1:183–188.
38. Rosenhouse-Dantsker, A., J. L. Sui, …, D. E. Logothetis. 2008. A sodium-mediated structural switch that controls the sensitivity of Kir channels to PtdIns(4,5)P_2. *Nat. Chem. Biol.* 4:624–631.
39. Lopes, C. M. B., H. Zhang, …, D. E. Logothetis. 2002. Alterations in conserved Kir channel-PIP2 interactions underlie channelopathies. *Neuron.* 34:933–944.
40. Rohács, T., C. M. Lopes, …, D. E. Logothetis. 2003. Specificity of activation by phosphoinositides determines lipid regulation of Kir channels. *Proc. Natl. Acad. Sci. USA.* 100:745–750.
41. Garneau, L., H. Klein, …, R. Sauvé. 2003. Contribution of cytosolic cysteine residues to the gating properties of the Kir2.1 inward rectifier. *Biophys. J.* 84:3717–3729.
42. Kuo, A., J. M. Gulbis, …, D. A. Doyle. 2003. Crystal structure of the potassium channel KirBac1.1 in the closed state. *Science.* 300:1922–1926.
43. Clarke, O. B., A. T. Caputo, …, J. M. Gulbis. 2010. Domain reorientation and rotation of an intracellular assembly regulate conduction in Kir potassium channels. *Cell.* 141:1018–1029.
44. Pegan, S., C. Arrabit, …, S. Choe. 2005. Cytoplasmic domain structures of Kir2.1 and Kir3.1 show sites for modulating gating and rectification. *Nat. Neurosci.* 8:279–287.
45. Nishida, M., and R. MacKinnon. 2002. Structural basis of inward rectification: cytoplasmic pore of the G protein-gated inward rectifier GIRK1 at 1.8 A resolution. *Cell.* 111:957–965.
46. Inanobe, A., T. Matsuura, …, Y. Kurachi. 2007. Structural diversity in the cytoplasmic region of G protein-gated inward rectifier K^+ channels. *Channels (Austin).* 1:39–45.
47. Nishida, M., M. Cadene, …, R. MacKinnon. 2007. Crystal structure of a Kir3.1-prokaryotic Kir channel chimera. *EMBO J.* 26:4005–4015.
48. Tao, X., J. L. Avalos, …, R. MacKinnon. 2009. Crystal structure of the eukaryotic strong inward-rectifier K^+ channel Kir2.2 at 3.1 A resolution. *Science.* 326:1668–1674.
49. He, C., X. Yan, …, D. E. Logothetis. 2002. Identification of critical residues controlling G protein-gated inwardly rectifying K^+ channel activity through interactions with the $\beta\gamma$ subunits of G proteins. *J. Biol. Chem.* 277:6088–6096.
50. Santiago, J., G. R. Guzmàn, …, J. A. Lasalde-Dominicci. 2001. Probing the effects of membrane cholesterol in the *Torpedo californica* acetylcholine receptor and the novel lipid-exposed mutation αC418W in *Xenopus* oocytes. *J. Biol. Chem.* 276:46523–46532.
51. Thompson, M. A. 2004. ArgusLab 401. Planaria Software LLC, Seattle, WA. ArgusLab 4.0.1. http://www.arguslab.com. Accessed December 21, 2010.
52. Joy, S., P. S. Nair, …, M. R. Pillai. 2006. Detailed comparison of the protein-ligand docking efficiencies of GOLD, a commercial package and ArgusLab, a licensable freeware. *In Silico Biol. (Gedrukt).* 6:601–605.
53. Fowler, P. W., A. Ivetac, …, M. S. P. Sansom. A database of potassium ion channel homology models and molecular dynamics simulations. http://sbcb.bioch.ox.ac.uk/kdb/. Accessed December 21, 2010.
54. Tai, K., P. J. Stansfeld, and M. S. Sansom. 2009. Ion-blocking sites of the Kir2.1 channel revealed by multiscale modeling. *Biochemistry.* 48:8758–8763.
55. Rosenhouse-Dantsker, A., and D. E. Logothetis. 2007. Molecular characteristics of phosphoinositide binding. *Pflugers Arch.* 455:45–53.
56. Haider, S., S. Khalid, …, M. S. Sansom. 2007. Molecular dynamics simulations of inwardly rectifying (Kir) potassium channels: a comparative study. *Biochemistry.* 46:3643–3652.
57. Xu, Y., H. G. Shin, …, Z. Lu. 2009. Physical determinants of strong voltage sensitivity of K^+ channel block. *Nat. Struct. Mol. Biol.* 16:1252–1258.
58. Tikku, S., Y. Epshtein, …, I. Levitan. 2007. Relationship between Kir2.1/Kir2.3 activity and their distributions between cholesterol-rich and cholesterol-poor membrane domains. *Am. J. Physiol. Cell Physiol.* 293:C440–C450.
59. Singh, D. K., A. Rosenhouse-Dantsker, …, I. Levitan. 2009. Direct regulation of prokaryotic Kir channel by cholesterol. *J. Biol. Chem.* 284:30727–30736.
60. Li, H., and V. Papadopoulos. 1998. Peripheral-type benzodiazepine receptor function in cholesterol transport. Identification of a putative cholesterol recognition/interaction amino acid sequence and consensus pattern. *Endocrinology.* 139:4991–4997.
61. Epand, R. M. 2006. Cholesterol and the interaction of proteins with membrane domains. *Prog. Lipid Res.* 45:279–294.
62. Gupta, S., V. N. Bavro, …, M. R. Chance. 2010. Conformational changes during the gating of a potassium channel revealed by structural mass spectrometry. *Structure.* 18:839–846.
63. Kuo, A., C. Domene, …, C. Vénien-Bryan. 2005. Two different conformational states of the KirBac3.1 potassium channel revealed by electron crystallography. *Structure.* 13:1463–1472.